A One-Dimensional Time-Dependent Model for the Vertical Stratification of the Upper Arctic Ocean

GÖRAN BJÖRK

Department of Oceanography, Gothenburg University, Gothenburg, Sweden

(Manuscript received 16 February 1988, in final form 28 June 1988)

ABSTRACT

A one-dimensional time-dependent model of the upper Arctic Ocean is presented. It describes the circulation above a dynamically passive reservoir of Atlantic water. The model is driven by freshwater runoff from land, ice production and export, Bering Strait inflow and wind. The mixed layer thickness is controlled by the shortest among the following three length scales: the depth to the upper pycnocline, the Ekman length and the Monin–Obukov length. The outflow is assumed to occur as geostrophically controlled coastal currents. Four integral quantities are defined in order to make objective comparisons between model generated and observed salt and temperature profiles.

The model generates a seasonally varying mixed layer in qualitative agreement with measurements. A halocline with water near the freezing temperature is also generated. This structure is sustained by the water coming from the Bering Strait. By comparing the model result with the observed freshwater content in the basin, likely values of the Bering Strait inflow Q_b and the ice export Q_i are found. These values are presented as an area in the Q_i, Q_b plane. It is shown that with this model, lacking shelf processes, it is impossible to obtain correct values for all integral quantities. The deviation between the computed and the observed stratification suggests that the Arctic Ocean has an internal source of salty water at temperature near the freezing point. This internal source of dense water is probably driven by ice production and the accompanying ejection of salt on the large shelf areas.

By introducing a hypothetical shelf with a prescribed distribution of outflow as a function of salinity it is possible to obtain nearly full agreement with the observed stratification. It is shown that the best fit is achieved when the volume flow from the shelf is in the interval $(1–1.5) \times 10^6$ m^3 s^{-1}.

1. Introduction

The Arctic Ocean with an area of about 9×10^6 km^2 consists of two major deep basins, the Canadian and the Eurasian with depths greater than 3000 m, surrounded by shallow shelf areas. The basins are separated by the Lomonosov ridge over which the depth is around 1000 m. The shelves occupy about one third of the total area. Especially at the Siberian coast the shelf is very wide, typically about 800 km. The Arctic Ocean is connected with adjacent seas by the Bering Strait, an open border in Barents Sea, the Fram Strait, and a number of narrow passages in the Canadian Archipelago (see Fig. 1).

In the Arctic Ocean, the conditions are greatly affected by the presence of sea ice. The ice is present during the whole year, except near the coasts during the summer. The ice thickness is greatest at the Northern Greenland and the Canadian coasts, about 6 m, and decreases towards the Siberia where the thickness is about 2 m (e.g., see Hibler 1979). More ice is produced during the winter than melts in the summer. This net production is exported, mainly through the Fram Strait.

The major features of the vertical structure in the Arctic Ocean can be described as follows (Treshnikov and Baranov 1973): On top there is a mixed layer of thickness between 25 and 50 m and temperature near the freezing point. The salinity increases horizontally from about 30‰ in the Beaufort Sea, to about 32‰ near the Fram Strait. Below the mixed layer is a halocline where the salinity increases to about 34‰ at 100 m depth, while the temperature is still near the freezing point. Below the halocline the temperature increases and forms a maximum with temperatures above 0°C. The layer with temperature above 0°C is called the Atlantic Layer. The salinity is here about 34.8‰. The upper boundary of the Atlantic layer is situated at about 300 m depth in the Beaufort Sea and rises to about 200 m near Greenland. The maximum temperature is between 0.4 and 1°C over most parts of the basin with the warmest water near the Fram Strait. The thickness of the Atlantic Layer is ranging between 800 and 500 m. Below the Atlantic layer the water is relatively homogeneous with temperature between 0 and −0.9°C, and salinity between 34.90 and 34.95‰. Figure 2 shows

Corresponding author address: Göran Björk, Department of Oceanography, University of Gothenburg, Box 4038, S-400 40 Gothenburg, Sweden.

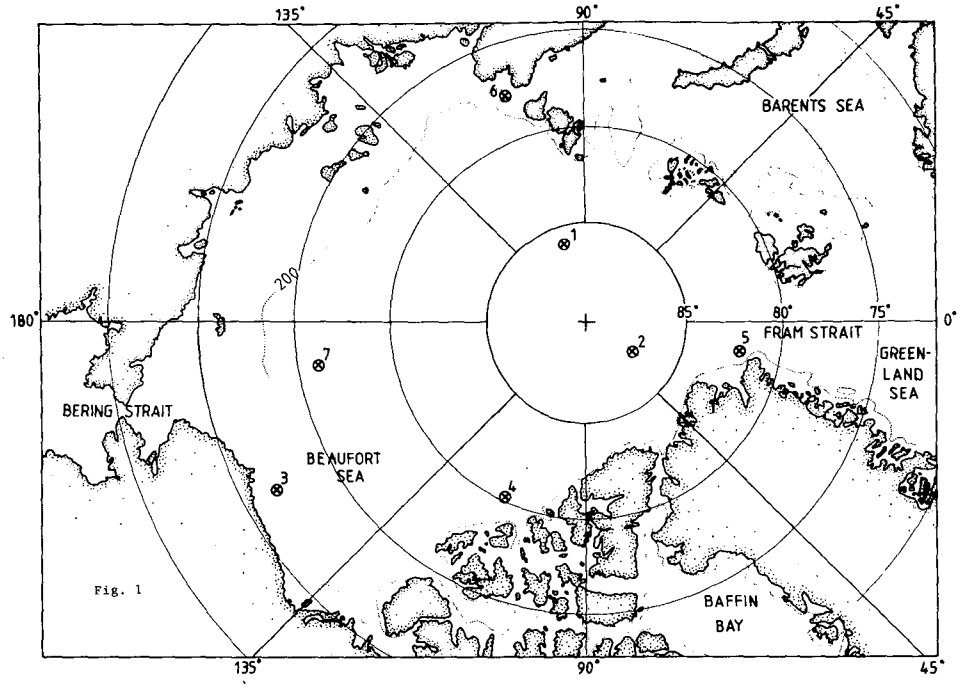

FIG. 1. Map of the Arctic Ocean.

profiles of salinity and temperature at the seven stations marked in Fig. 1.

The Arctic Ocean receives water mainly by runoff from land, inflow of relatively low-saline water of Pacific origin through the Bering Strait and inflow of Atlantic water through the Fram Strait in the West Spitsbergen current. Atlantic water enters also through the open border to the Barents Sea. Water leaves the basin mainly via the Fram Strait and the Archipelago. The flux of Arctic Ocean surface water through the Barents Sea border seems to be of minor importance (Rudels 1987). The magnitude of the various fluxes is a major concern of the present paper.

The origin of the halocline in the Arctic Ocean has been the subject of an extensive discussion during the last decade (see for example Aagaard et al. 1981). Since it is impossible to create the halocline water by local mixing of the surface water with the underlying Atlantic water, the halocline must be maintained by some different mechanism. A possible candidate is that the water in the halocline is advected into the basin. Such water may be created by the ice generation on the shelves during the winter (Aagaard et al. 1981). As pointed out later in this paper winter water from the Bering Strait may sustain at least a part of the halocline.

Some models dealing with the hydrographical conditions in the Arctic Ocean have been developed during the last years. Stigebrandt (1981) developed a steady-state two layer model including a heat budget. In this model the stratification is represented by a brackish layer above a passive reservoir of Atlantic water. The ouflow is assumed to occur as geostrophically controlled coastal currents through the Fram Strait and the Archipelago. The vertical mixing in the system is described by an entrainment process. The main purpose with that model was to establish a relation between the ice thickness and some external parameters, for example, the runoff.

Killworth and Smith (1984) developed a steady state, one-dimensional model including separate treatment of the shelves. This model is focused upon the halocline problem. The mixing is described by a diffusion equation, and the dynamics within the Atlantic layer is considered. This model is able to generate the Arctic mixed layer and shows the importance of the water coming from the Bering Strait in retaining the halocline. The result at lower levels, however, deviated much from the observed temperature and salt profiles.

The model described in the present paper is time-dependent and one-dimensional. It can be seen as a further development of the dynamical part (without heat budget) of Stigebrandts two layer model. The same kind of geostrophic outflow parameterization is used. The Atlantic layer is also here treated as a passive reservoir. The mixed layer is modeled using the seasonal pycnocline model in Stigebrandt (1985). The purpose of developing the present model was to describe more of the observed phenomena in the upper Arctic Ocean than is possible using a two layer steady-state model. It is shown below that this model reproduces the qualitative behavior of the observed seasonal cycle of the mixed layer. A cold halocline that originates from the Bering Strait inflow is also generated. Using this model one may determine the possible combinations of the

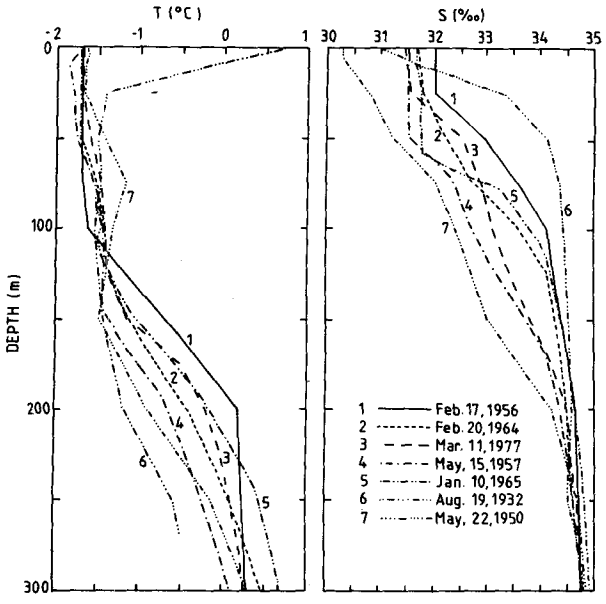

FIG. 2. Vertical profiles of temperature and salinity at the seven locations shown in Fig. 1. From Aagaard et al. (1981) and NODC data bank.

ice export, the transport through the Bering Strait and the freshwater runoff from land. In the literature one may find combinations which are incompatible with the model results and with continuity requirements.

With the present model it is however not possible to obtain full agreement between the computed and the observed temperature and salinity stratification. This departure shows clearly that the stratification in the Arctic Ocean to a large extent is maintained by processes not included in the model. A likely missing process is the circulation induced by ice formation and salt rejection on shallow shelves. An experiment is carried out where a hypothetical shelf with specified outflow is coupled to the model. It is shown that the inclusion of shelf circulation makes it possible to obtain good agreement between model results and observations.

The model is described in section 2, where some integral test quantities are also defined. Section 3 deals with the various inputs (forcing) that are used. Time dependent and steady state behavior of the model is presented in section 4. In section 5, the model results are compared with the measurements. In section 6 the hypothetical shelf is coupled to the original model. Finally, in section 7, some weaknesses of the model are discussed together with possible future improvements.

2. Model description

The model describes the upper few hundred meters of the Arctic Ocean without considering the topography (vertical side walls). It is one-dimensional and time-dependent. The model is forced by runoff, Bering Strait inflow, ice production and wind. The fact that there are only weak horizontal gradients of temperature and salinity within the real system (see above) indicates that a one-dimensional model should be able to generate a realistic first-order description of the stratification.

The structure of the model is outlined in Fig. 3. On top of a stratified water column there is an ice sheet of thickness h_i. The model description of the water column below the ice can be separated into three parts. Just below the ice there is a well mixed layer of temperature T_m (the freezing point) and salinity S_m. Below the mixed layer there is a transition layer where the temperature $T(z)$ and salinity $S(z)$ gradually attains the values in the Atlantic Layer. Two different lengths are used describing the mixed layer thickness: h, defined as the distance between the free water surface and the bottom of the mixed layer and h_w, defined as the distance between the lower surface of the ice sheet and the bottom of the mixed layer. In the Atlantic layer the temperature T_a and salinity S_a are set constant. Thus, the model only describes the dynamics above the Atlantic layer.

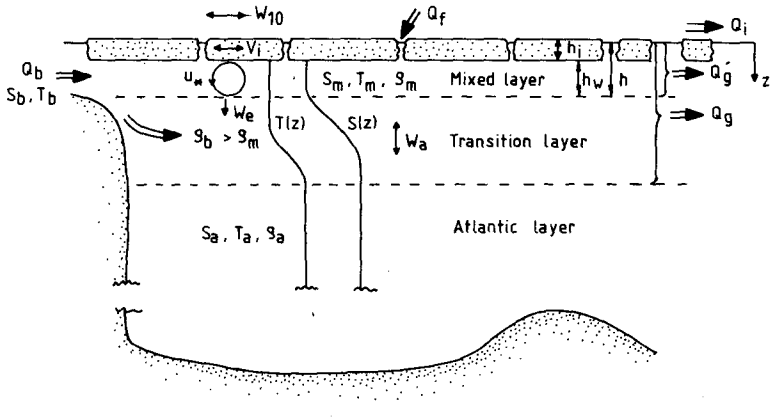

FIG. 3. Schematic structure of the model.

Also sketched in Fig. 3 are the different fluxes into and out of the basin: the freshwater supply Q_f, the inflow through the Bering Strait Q_b (of salinity S_b and temperature T_b), the ice export Q_i, the outflow of mixed layer water Q_g' and the total outflow above the Atlantic layer Q_g. The Bering Strait inflow enters at the sea surface or is injected at the level of neutral buoyancy, depending on whether the density of the inflow is less or greater than the mixed layer density.

The ice production/melting cycle in the Arctic is expressed by the parameter P_i which is positive when the ice is growing and negative during melting conditions. In the Arctic more ice is produced during the winter than melts in the summer. The ice export is set equal to the annual net production. Thus, the total amount of ice in the model is constant on a long term time scale.

The mixed layer is maintained by the combined action of wind generated mixing, thermohaline processes (at the sea surface), and advection resulting from the inflows and outflows. Due to the presence of pack ice, the action of the wind on the mixed layer can be considered as a two step process: The wind stress causes an ice velocity V_i which in turn generates a stress, proportional to the square of a friction velocity u_*, in the mixed layer. Convection arises when salt is ejected from the growing ice. The mixing across the bottom of the mixed layer is described by the entrainment velocity w_e, defined as the speed of the downward penetration of the mixed layer.

Below the mixed layer properties can change by vertical advection, injection of water coming from the Bering Strait and diffusion. The advection is described by the velocity w_a. For example, the outflow generates a negative w_a, which is equivalent to a movement of the isolines towards the sea surface.

a. Model equations

The mixed layer dynamics, follows largely a pycnocline model developed by Stigebrandt (1985). In that model, there are conservation equations for the mixed layer thickness, temperature and salinity, and a parameterization for the entrainment velocity. From volume conservation the equation for the Arctic Ocean mixed layer thickness is

$$\frac{dh}{dt} = (\mu Q_b + Q_f + \epsilon Q_i + Q_g')\frac{1}{A} + w_e \qquad (1)$$

where A is the area of the basin, and ϵ is the ratio between the ice and water densities. All the transports are taken positive when adding volume to the basin. The behavior of the Bering Strait flow is described by the parameter μ which can take the value 0 or 1 according to

$$\mu = \begin{cases} 1, & \rho_b \leq \rho_m \\ 0, & \rho_b > \rho_m. \end{cases}$$

Thus, Eq. (1) shows that the mixed layer depth can change by the various advective volume fluxes into and out from this layer, and by the turbulent entrainment of water from below. There are, however, occasions which will be discussed later, when Eq. (1) is not valid and the mixed layer thickness is controlled by other mechanisms. Among the terms on the right hand side of (1), Q_f and Q_b are given as input (forcing) to the model, while w_e, Q_i and Q_g' are computed. Here Q_f, Q_b and w_e are always positive, while Q_i and Q_g' are always negative. The ice export is equal to the mean ice production according to

$$Q_i = -A\overline{P_i} \qquad (2)$$

where the overbar denotes an annual average. The ice production P_i will be prescribed as an external forcing parameter. The parameterizations of w_e and Q_g are discussed below.

The sea level is held constant in the model. Therefore, an inflow to the mixed layer always causes a positive vertical velocity at the bottom of the layer. This vertical advective velocity actually remains all the way down to the Atlantic layer. The salt balance for the mixed layer reads:

$$\frac{dS_m}{dt} = \{[\mu Q_b(S_b - S_m) - Q_f S_m]/A + \epsilon P_i(S_m - S_i) + w_e(S(h) - S_m)\}/h_w \qquad (3)$$

where $S(h)$ is the salinity just below the mixed layer. Equation (3) shows that the salinity of the mixed layer can be changed by the Bering Strait inflow, freshwater supply, ice production and entrainment. Because the mixed layer temperature is set constant (at the freezing point) in this model there is no need for a mixed layer temperature equation. The fraction of the water column that consists of ice should be excluded in the salt balance. Therefore, the mixed layer thickness h_w is used in Eq. (3). The relation between h_w and h is

$$h_w = h - \epsilon h_i. \qquad (4)$$

Changes of the ice thickness are given by the ice mass balance equation:

$$\frac{dh_i}{dt} = P_i + Q_i/A. \qquad (5)$$

Following Stigebrandt (1985), the dynamics of the mixed layer depends on which among the following three length scales is the shortest: 1) the distance to the upper pycnocline h, 2) the Monin–Obukov length and 3) the Ekman length. When h is the shortest length scale the entrainment velocity is given by the formula:

$$w_e = (2m_0 u_*^3/h_w - kB)/g',$$

$$g' = g(\rho(h) - \rho_m)/\rho(h) \qquad (6)$$

where $\rho(h)$ is the density just below the pycnocline and u_* is the friction velocity in the mixed layer. When ice

is present the friction velocity is related to the ice velocity according to the equation:

$$u_*^2 = C_{di}V_i^2 \tag{7}$$

where C_{di} is an ice–water drag coefficient and V_i is the ice velocity. There is also a need for a relation between ice velocity and wind velocity. This relation is taken from Thorndike and Colony (1982) who fitted a linear relation between the wind at 10-m height and the ice velocity.

$$V_i = a_0 W_{10} \tag{8}$$

The constant m_0 in Eq. (6) will be related to a Richardson flux number R_f and the drag coefficient according to

$$m_0 = R_f/\sqrt{C_{di}}. \tag{9}$$

Taking $R_f = 0.05$ and $C_{di} = 5.5 \times 10^{-3}$ one obtains $m_0 \approx 0.7$, which is close to the value 0.6 that Stigebrandt (1985) calculated using temperature data from the Baltic Sea. In Eq. (6) B is the buoyancy flux through the sea surface. When B is positive the entrainment velocity is suppressed. For negative B there is convection in the mixed layer acting as an extra energy source for mixing. Only a fraction of this energy (5%) is assumed to be used for mixing. This behavior of the buoyancy flux is described by the parameter k: $k = 1$ when $B \geq 0$, $k = 0.05$ when $B < 0$. The buoyancy flux is given by the expression:

$$B = g\beta\{[Q_f S_m + \mu Q_b(S_m - S_b)]/A - \epsilon P_i(S_m - S_i)\}, \quad \beta = \frac{1}{\rho}\frac{\partial \rho}{\partial S} \tag{10}$$

Thus, the buoyancy sources for the mixed layer are: the freshwater supply, the Berings Strait inflow (if this water is less dense than the water in the mixed layer) and the ice production/melting. Due to the fact that the mixed layer is kept at the freezing temperature, the heat exchange with the atmosphere is accounted for in the ice production term.

When the buoyancy flux is large and positive, the entrainment velocity can formally change sign and become negative. This is not physically possible, consequently Eq. (6) is only valid when $w_e > 0$. When w_e becomes formally negative the shortest of the Ekman length h_e and the Monin–Obukov length h_m will control the thickness of the mixed layer:

$$h_e = Ku_*/f \tag{11}$$

$$h_m = 2m_0 u_*^3/B \tag{12}$$

where K is an empirical constant. The value of K has been estimated to 0.2 by Stigebrandt (1985) using Baltic data and this value is also used here.

The outflow Q_g is assumed to occur as geostrophically balanced coastal currents with the underlying Atlantic water at rest. This approach was also used by Stigebrandt (1981) in his two layer model for the Arctic Ocean. According to Stigebrandt there are two main "geostrophical outlets": one in the Fram Strait and one in the Lancaster Sound in the Canadian Archipelago. The latter area also includes a number of minor channels. Stigebrandt (1981) estimated the total number of outlets, γ, to be about 2.3. Using recent estimates of the transports through the different outflow areas it is however possible to get other values of γ. In the present model the number of such "geostrophical outlets", among other things affecting the total outflow (see discussion below), is described by the parameter λ. The model was run with different λ between 0.9 and 2.0.

An estimate of the transport at each level in a geostrophical outlet can be obtained by integrating the thermal wind equation across the flow. The stratification in an outflow area is sketched in Fig. 4 where the coast is located at $x = 0$. The stratification at the coast (shown separately in the figure) is assumed to be the same as in the central Arctic. Far off the coast, at $x = x_a$, the stratification is absent. A front is located somewhere at $0 < x < x_a$. When the density is equal to the Atlantic density, ρ_a, the water is assumed to be at rest. The thermal wind equation reads:

$$\frac{\partial v}{\partial z} = \frac{g}{\rho_a f}\frac{\partial \rho(x, z)}{\partial x} \tag{13}$$

where v is the coast-parallel velocity in the y direction. Integrating (13) in the x-direction from $x = 0$ to $x = x_a$ gives

$$\frac{\partial q(z)}{\partial z} = \frac{g}{\rho_a f}(\rho_a - \rho(z)) \tag{14}$$

where $\rho(z)$ is the density at the coast and

$$q(z) = \int_0^{x_a} v\,dx; \tag{15}$$

$q(z)$ is then the transport per unit depth across the outflow region. Integrating (14) in the z-direction from z to a level H_m (where $\rho = \rho_a$) in the Atlantic layer, and using the requirement that $v = 0$ when $\rho = \rho_a$ gives

$$q(z) = -\frac{g}{\rho_a f}\int_z^{H_m} (\rho_a - \rho(z))dz. \tag{16}$$

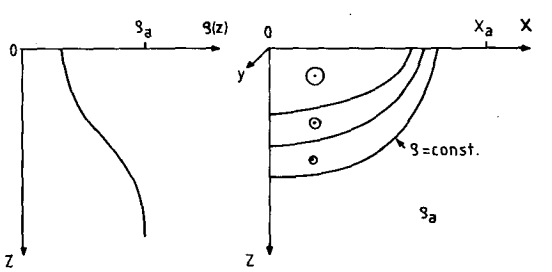

FIG. 4. Schematic sketch of a geostrophic outlet (right). The density profile at the coast $\rho(z)$ is shown separately (left).

By integrating Eq. (16) from $z = 0$ to z one obtains the transport $Q_T(z)$ above the level z:

$$Q_T(z) = \int_0^z q(z)dz. \tag{17}$$

Integrating over the whole water column to $z = H_m$ gives the total transport in each geostrophical outlet. This method to compute the baroclinic flow from a stratified "pool" was used by Stigebrandt (1987).

The total transport out from the basin above level z, taking all outlets into account, is obtained by multiplying $Q_T(z)$ with the number of outlets λ. The total outflow from the basin Q_g and the outflow from the mixed layer Q'_g can then be expressed:

$$Q_g = \lambda Q_T(z = H_m) \tag{18}$$

$$Q'_g = \lambda Q_T(z = h) \tag{19}$$

The advective vertical velocity at level z, w_a, inside the basin is related to the different in and outflows according to

$$w_a(z) = \begin{cases} (\lambda Q_T(z) + Q_f + \epsilon Q_i)/A, & z \leq z_b \\ (\lambda Q_T(z) + Q_f + \epsilon Q_i + Q_b)/A, & z > z_b \end{cases} \tag{20}$$

where z_b is the level at which the Bering Strait water is injected. Finally, below the mixed layer the local rate of change of the salinity and the temperature are

$$\frac{\partial S}{\partial t} = w_a \frac{\partial S}{\partial z} + \kappa \frac{\partial^2 S}{\partial z^2} \tag{21}$$

$$\frac{\partial T}{\partial t} = w_a \frac{\partial T}{\partial z} + \kappa \frac{\partial^2 T}{\partial z^2} \tag{22}$$

where κ is a constant vertical diffusivity. The model is normally run with $\kappa = 0$. However, even in this case there are in fact nonzero diffusive fluxes because the vertical advection in connection with the model grid generates "numerical" diffusion. The magnitude of this is estimated below and is found to be less than, or possibly of the same order as, the diffusion in the real system.

The values of the different constants used in the model are summarized in Table 1. This completes the mathematical formulation of the model. Given the different imposed fluxes and initial conditions, the above set of equations can be used to generate time dependent salinity and temperature profiles.

TABLE 1. Values of constants used in the model.

A	0.9×10^{13} (m^2)
g	9.81 (m s^{-2})
f	1.43×10^{-4} (s^{-1})
C_{di}	5.5×10^{-3}
Rf	0.05
K	0.2
ϵ	0.9
Ct	4.18×10^3 (J (kg °C)$^{-1}$)
S_i	5 (‰)
S_a	34.8 (‰)
T_a	0.5 (°C)

b. *Definition of some test quantities*

Having a model that generates continuous salt and temperature profiles there is need for some integral quantities when comparing the model results with the observations. These quantities should describe the major features of the profiles but not necessarily all the details. Four integral quantities describing the state of the system were chosen (cf. Gill and Turner 1976). The first two are the freshwater content HF and the heat deficit HD, defined as

$$\mathrm{HF} = \int_0^{H_m} (S_a - S)/S_a dz \tag{23}$$

where HF is the volume of freshwater in the liquid phase per unit area, or simply the height of the freshwater column. The upper integration limit used here neglects the fact that the uppermost part of the water column actually consists of ice. The error introduced by choosing this simplified integration limit is only about 0.1 meter of freshwater per meter of ice.

$$\mathrm{HD} = Ct\rho_a \int_0^{H_m} (T_a - T)dz \tag{24}$$

where Ct is the specific heat, and T_a is the temperature in the Atlantic layer. Then HD is the energy per unit area needed to heat the whole water column, ice not accounted for, to the temperature of the Atlantic water.

The two quantities above specify only the content of freshwater and heat, giving no information about the vertical distribution of the salinity and temperature. The vertical distributions are roughly described by the two quantities SM and TM, defined as

$$\mathrm{SM} = \int_0^{H_m} (S_a - S)/S_a z dz \tag{25}$$

$$\mathrm{TM} = \int_0^{H_m} (T_a - T)/T_a z dz. \tag{26}$$

These two quantities can be used in the following way: if, for example, HF calculated by the model is in agreement with the measurements but the layer with fresher water is thicker than the measurements indicate, SM will be too large.

Together with these integral quantities also the mixed layer thickness h and salinity S_m will be compared with the data.

If the density in the system is controlled by the salinity (temperature), SM (TM) will be proportional to the potential energy PE of the system respectively. In the Arctic Ocean the density is mainly controlled by the salinity and PE $\approx g\rho_0\beta S_a$SM, where ρ_0 is the density of freshwater. PE is interesting in connection with the total outflow Q_g from the system because Q_g is closely related to PE.

3. External forcing and fluxes

a. Runoff

The annual mean freshwater supply to the Arctic Basin due to runoff is about 0.1 Sv (1 Sv $\equiv 1 \times 10^6$ $m^3 s^{-1}$) (e.g., see Andersson et al. 1983). Values of the mean runoff found in the literature do not vary much. The seasonal variability is however large (SCOR 1979) with about ten times higher values during summer compared to winter. The net precipitation seems to be rather low compared to the river discharge (SCOR 1979). In the model calculations the mean freshwater supply was 0.11 Sv, with an annual cycle as shown in Fig. 5.

It might seem a bit curious to use seasonal variation in the forcing from the boundaries (e.g., the runoff) because the seasonal variation caused by this type of forcing will be very small, or eventually not detectable at all, in the central parts of the real basin. In order to generate a seasonal signal in the middle of the basin, the water from the boundaries must move about 1000 km in a few months, say 100 days. This implies an advective velocity of about 0.1 m s^{-1}. This seems quite high for most parts of the Arctic Ocean. However, near the coasts a large seasonal signal will be seen, and consequently the horizontal mean over the basin must be seasonal-dependent. This justifies the time-dependent boundary forcing because horizontal means is just what a one-dimensional model is able to reproduce.

b. Ice production

Due to the insulating effect of the ice, the ice production is largely dependent on ice thickness. Arctic pack ice is indeed very irregular in thickness, ranging from zero in leads to maybe 30 m in pressure ridges. Thus, one can expect large variations in ice production both in space and time. The various processes that control ice production are not incorporated in this version of the model. Instead, in order to get a reasonable annual variation of the ice production as input for the model, monthly values were taken from Hibler (1979).

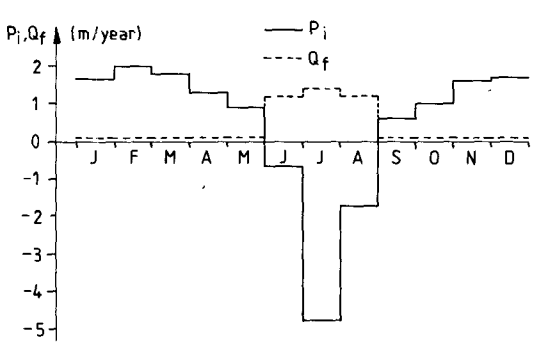

FIG. 5. The freshwater supply and the ice production (m yr^{-1}) each month of the year used in the model calculations. The mean freshwater supply is 0.11 Sv or 0.38 m yr^{-1} (based on $A = 9 \times 10^6$ km^2).

The annual cycle of ice production is shown in Fig. 5. The growth rate is largest in February (2 m yr^{-1}) and the melting is largest in July (−4.8 m yr^{-1}). The annual mean is $P_i = 0.46$ m yr^{-1}, corresponding to an ice export of 0.13 Sv (based on $A = 9 \times 10^6$ km^2). Among other estimates of the ice export, one may mention 0.16 Sv (Vinje and Finnekåsa 1986), and 0.08 Sv (Rudels 1987). In the model calculations, the ice production was varied by adding a constant to the ice production curve in Fig. 5 so that the associated ice export varies between 0.07 and 0.17 Sv.

c. Bering Strait inflow

The magnitude of the inflow through the Bering Strait has been estimated to be between 1.5 (Aagaard and Greisman 1975) and 0.6 Sv (Aagaard et al. 1985). In the model calculation, the Bering Strait inflow was varied between 0 and 1.8 Sv. The flow rate was set constant during the year because the uncertainty of the actual magnitude of this inflow do not justify a time-dependent flux.

The salinity and temperature in the Bering Strait water can be considered to be known more accurate than the volume flux. Figure 6 shows monthly means of salinity and temperature for all stations taken after 1950 in the Bering Strait area 64°–65°N, 166°–173°W (from the NODC hydrographic database). The salinity shows an annual variation with high values during the spring and low during the autumn. For the model computations this salinity and thereby density variation is quite important because the inflow will influence the properties in the basin over a much wider depth range than a single density inflow would do.

The number of observations for each month (indicated in the figure) varies a lot during the year with a large number in the summer and no observations at all in December and January. Therefore, the reliability of the mean values also varies. The values in Fig. 6 were however used to estimate the mean salinity (32.2‰) and the amplitude of the annual variation (0.6‰). A sine curve with this mean value and amplitude was adopted (dotted line in the figure), as input for the model computations.

The freshwater fraction of the Bering Strait inflow is about $0.075Q_b$, using $S_a = 34.8$‰ as reference salinity and $S_b = 32.2$‰. For the largest Q_b-values used in the model computations, this source of freshwater is as large as the runoff.

The temperature of the Bering Strait water shows also a seasonal cycle with values near the freezing point

during winter and higher during summer. Traces of this summer water can be seen in the Beaufort Sea area (Treshnikov and Baranov 1973) as a warmer layer at about 100 m depth, but the temperature is still below −1°C.

The Bering Strait water will certainly lose part of its summer heat both to the atmosphere and to ice melting during the travel across the wide Chukchi shelf. The amount of heat actually lost is however hard to estimate. The model predictions of the temperature maximum caused by the Bering Strait summer water will therefore be rather uncertain.

However, the mean summer temperature on the Chukchi Sea side of the Bering Strait (68°–72°N, 165°–175°W) is generally about 1°C lower than on the Bering Sea side. The observed mean summer temperature is probably also biased because most measurements are probably taken during especially warm summers with light ice conditions allowing ship traffic. Therefore a maximum summer temperature of 2°C was adopted as representative for the Bering Strait. The temperature forcing used in the model for the whole year is shown in Fig. 6.

d. Wind forcing

The wind data was taken from NCDC Pilot Chart data file, which contains monthly means for several cli. ıate parameters in so-called Marsden squares. The parameters used for the mixing wind calculations are W: mean windspeed, SDA: standard deviation and N: number of observations. The mixing wind is dependent on W and SDA and is estimated in the following way:

$$W_{10} = (W^3 + 3W(\mathrm{SDA})^2)^{1/3}. \qquad (27)$$

The Arctic mixing wind for each month was then calculated, taking the mean value of all the estimates of the local mixing wind in Marsden squares 263–288 and 901–936 for which N was greater than 50. The

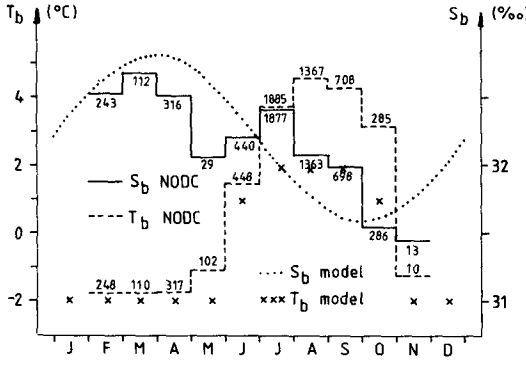

FIG. 6. The salinity S_b and temperature T_b in the Bering Strait area (64°–66.5°N, 166°–173°W) each month of the year. Spatial means from the NODC data bank. The number of observations associated with each mean value is also shown. The dotted sine curve and the crosses shows S_b and T_b values used in the model calculations.

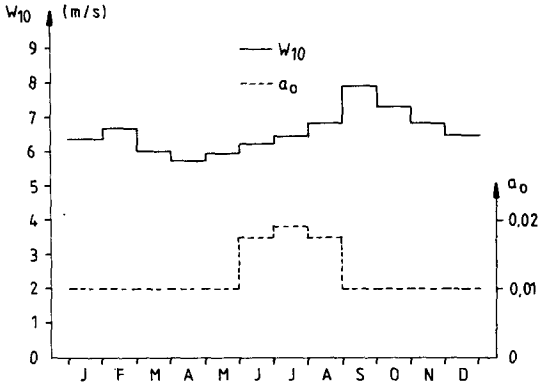

FIG. 7. The mixing wind W_{10}, and the air–ice velocity parameter a_0, each month of the year, used in the model calculations.

annual cycle of the mixing wind is shown in Fig. 7 together with the parameter a_0 that is used in the relation between wind speed and ice speed. This parameter is larger during the summer when there is more open water and the pack ice has lower internal stress (Colony and Thorndike 1982).

4. Time dependent and steady state behavior of the model

The model was run for different combinations of Q_i, Q_b and λ simulating 100 years. The time step was one day, and the vertical resolution 2 meters. During the model run, the annual means for HF, HD, SM, TM, S_m, h and Q_g were calculated. The system reaches steady state after about 30 years (e-folding time scale). Thus, a 100-year long simulation seems to be sufficient.

a. Time dependent properties of the model

Superposed upon the steady state, the system has an annual cycle which is most pronounced for salinity. In order to visualize this cycle, bimonthly salinity and temperature profiles are shown in Fig. 8 for the case $(Q_i, Q_b, \lambda) = (0.1\ \mathrm{Sv}, 1.0\ \mathrm{Sv}, 1.5)$. As it appears from this figure, the mixed layer is fresher and thinner in summer than during winter. This seasonal variation is mainly caused by variations in the buoyancy flux B. When B turns positive early in the summer (because of large fresh water supply from land and ice melting) the mixed layer retreats quickly, and a new halocline is created at a more shallow depth (the Ekman depth). This thin mixed layer receives all of the freshwater, which decreases the salinity there. When B turns negative again in the autumn the mixed layer starts to deepen and the salinity increases due to entrainment of saltier water from below and ejection of salt from the growing ice. A behavior of the mixed layer properties similar to that displayed in Fig. 8 has been observed in the Arctic. Figure 9 shows the mixed layer

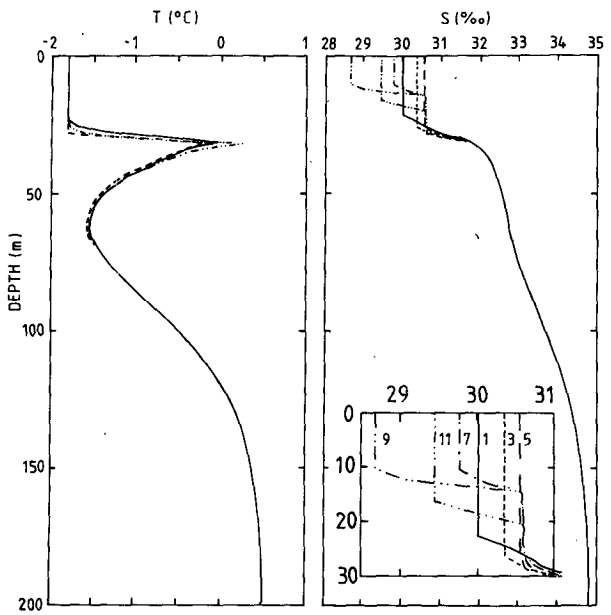

FIG. 8. Profiles of salinity and temperature every second month of the year as a result from model calculations, for the case (Q_i, Q_b, λ) = (0.1 Sv, 1.0 Sv, 1.5).

thickness and salinity during one year in the Beaufort Sea (from Lemke and Manley 1984). Note the rapid decrease of the mixed layer thickness in the early summer and the slow increase during winter.

The temperature maximum (minimum) in the upper parts of the water column are generated by the Bering Strait summer (winter) water, respectively. It is interesting to note that a realistic halocline structure (i.e., temperature near the freezing point at depth far below the mixed layer) is produced by the winter water. The profiles in Fig. 8 therefore strongly indicate that at least the winter water coming from the Bering Strait is capable of maintaining a part of the halocline structure in the Arctic Basin.

The temperature maximum for the case shown in Fig. 8 is unrealistically high considering that temperatures above −1°C are hardly ever observed even in the Beaufort Sea, which is close to the heat source. The temperature maximum is, as will be shown below, very sensitive to the maximal mixed layer density. In the case shown in Fig. 8 nearly all Bering Strait summer water is injected below the maximum depth of the mixed layer. Most of the summer heat is then stored in the water column. If the maximal mixed layer density is greater than the density of the Bering Strait summer water, some of the summer water will be entrained into the mixed layer during autumn–winter and that heat will be lost.

The four integral quantities HF, HD, SM and TM show small variations during the year. For example, the annual variation of HF is only 0.6 m for a realistic parameter combination.

b. Steady state response of the model to variations in Q_b, Q_i and λ

Before making a quantitative comparison between model results and field data it seems valuable with a brief discussion of the response of the system when varying the different imposed fluxes and λ. Figures 10–12 show annual means of HF, HD, SM, TM, S_m, h, and Q_g for different values of Q_i, Q_b and λ. Although the lowest estimate of Q_b found in the literature is about 0.5 Sv, the case $Q_b = 0$ is also shown. κ is always zero if nothing else is told.

Starting with the λ-dependence Fig. 10 shows that HF, HD, SM and TM all increases with decreasing λ. When λ is changed from $\lambda = 2$ to $\lambda = 1$ the outflow decreases for a given upstream stratification. The potential energy (proportional to SM) must then be larger in order to establish balance between the volume fluxes into and out from the system. A larger SM will also be reflected by a larger HF. When HF and SM become larger the generally low temperature Bering Strait inflow will be injected further down in the water column and thereby increasing both HD and TM.

The freshwater content HF (Fig. 10a) increases with Q_b because of the low salinity of the Bering Strait inflow. When Q_i increases, more freshwater is removed as ice and HF decreases. For sufficiently low values of Q_b and high Q_i, HF vanishes since the inflow of freshwater is less than the outflow as ice. In this regime the model breaks down because the mixed layer thickness will be infinite. Figure 10a shows clearly that the Bering Strait inflow has a large buffering effect on the system when increasing Q_i. The system can sustain much larger ice export when Q_b is for example 0.5 Sv compared to the case $Q_b = 0$. The heat deficit (HD) (Fig. 10b) is strongly dependent on Q_b due to the generally low temperature of this inflow. HD increases with increasing Q_i since the water column will be denser causing interleaving of Bering Strait summer water closer to the surface where a larger part of it will be entrained during the autumn–winter mixed layer deepening. The first mo-

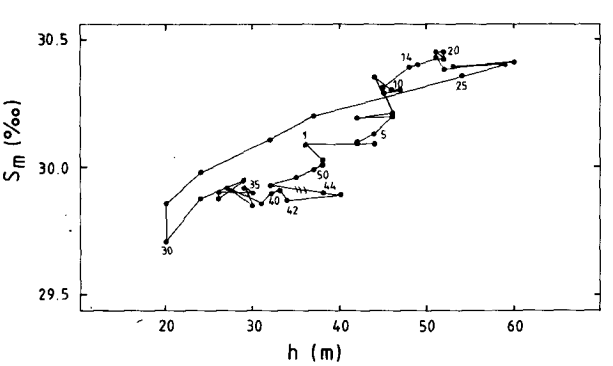

FIG. 9. Mixed layer salinity and depth each week during one year from measurements in the Beaufort Sea (from Lemke and Manley 1984). The numbers shown are week number.

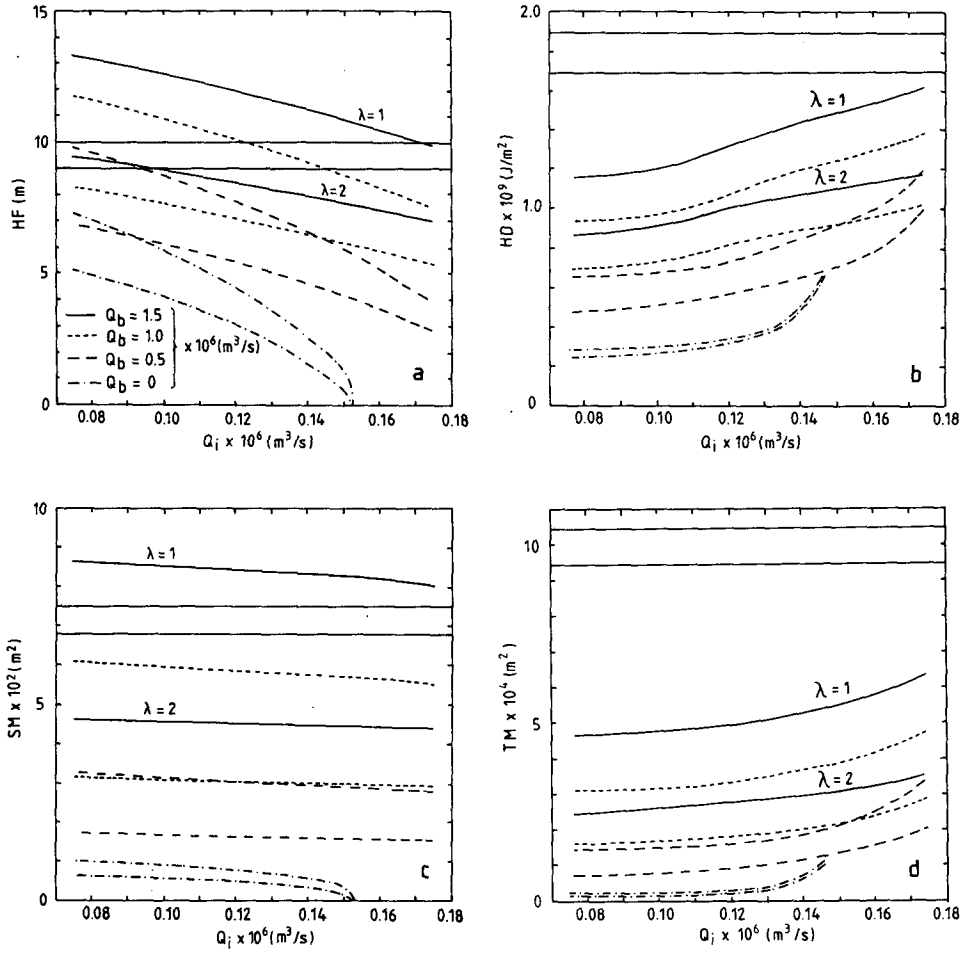

FIG. 10. Model result showing (a) the freshwater content HF, (b) the heat deficit HD, (c) first moment of salinity SM and (d) first moment of temperature TM for different Q_i, Q_b and λ. The upper curve of the same type shows the case $\lambda = 1$, the lower curve the case $\lambda = 2$. Also shown for each quantity is the range (between the horizontal lines) obtained from measurements in the Arctic Ocean (data range).

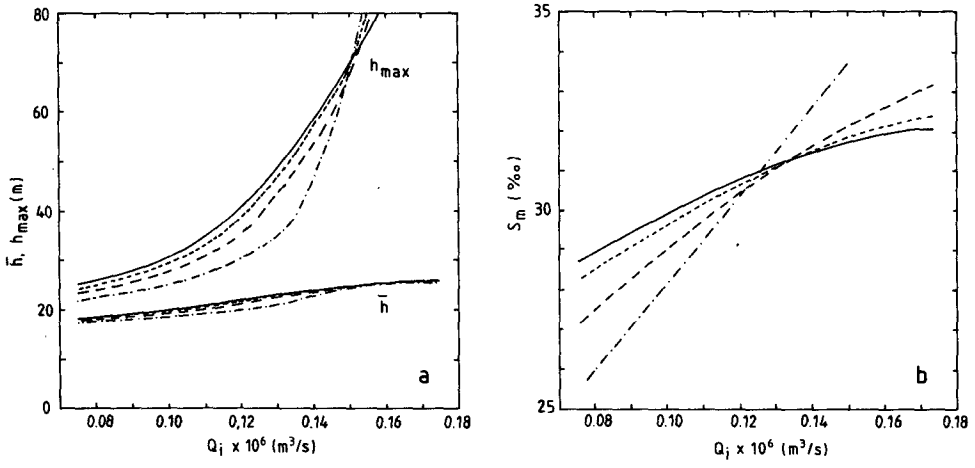

FIG. 11. Model result showing (a) the annual mean thickness $\bar{h}$ (lower four curves), and the annual maximum thickness h_{max} (upper four curves) of the mixed layer and (b) the annual mean of the mixed layer salinity S_m for different Q_i, Q_b and $\lambda = 1.5$. The different type of lines represents different values of Q_b (see Fig. 10 for identification).

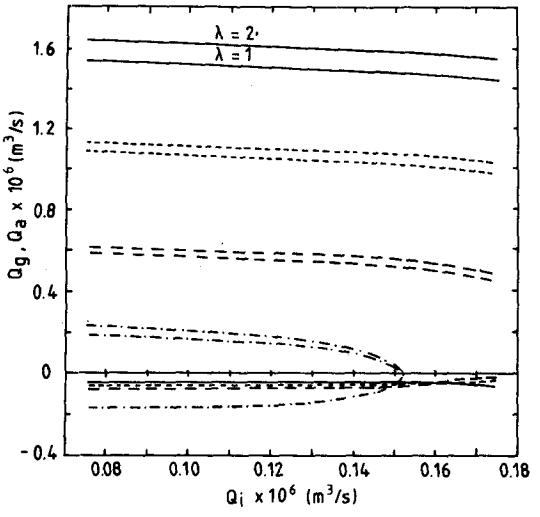

FIG. 12. Model result showing the total outflow Q_g (positive values) and the Atlantic inflow Q_a (negative values) for different Q_i, Q_b and λ. The different type of lines represents different values of Q_b (see Fig. 10 for identification). Upper curve of the same type represents λ = 2 and lower curve λ = 1. For Q_a, only λ = 1.5 is shown.

ment of salinity and temperature SM, TM (Fig. 10c, d) shows generally the same behavior as HF and HD.

The annual mean of the mixed layer depth h and salinity S_m (Fig. 11) increases with increasing Q_i as can be expected. The variations in mixed layer depth are not so large with respect to Q_b because the inflow from the Bering Strait mainly enters below the mixed layer. The mixed layer properties are therefore only affected indirectly by Q_b. Also shown in Fig. 11a is the annual maximum of the mixed layer depth. The mixed layer salinity shows an interesting behavior, namely that S_m increases with Q_b for low values of Q_i and decreases with increasing Q_b for high values of Q_i. This is due to the fact that for low values of Q_i the Bering flow acts to make the pycnocline less sharp so that the mixing can reach further down, increasing S_m. For large Q_i the buffering effect of Q_b starts to act and S_m becomes lower when increasing Q_b.

In Fig. 12 the total outflow Q_g is shown as function of Q_i, Q_b and λ; Q_g is almost unchanged when varying the outflow parameter λ, because the outflow just balances the net inflow to the system. Instead Q_g is closely related to the strength of the Bering Strait inflow, with values just a bit higher than Q_b. Remembering that the freshwater supply and the ice export nearly cancel, the near "equality" between Q_g and Q_b indicates that upward mixing (and inflow) of Atlantic water within the system is rather small. The explanation for this is that the mixing in the system mainly is between the mixed surface layer and the Bering Sea water in the halocline. Thus, the water coming from the Bering Strait acts as a barrier between the surface and the Atlantic layer. This can be seen in Fig. 8 where the deepest mixing never reach down to the Atlantic layer. Theoretically, the upward mixing of Atlantic water should be exactly zero when $\kappa = 0$ and the mixing does not reach down below the Bering Strait water. However, the numerical diffusion makes the inflow of Atlantic water become nonzero.

The Atlantic inflow Q_a can be calculated using the continuity equation for the whole system in steady state:

$$Q_a + Q_g + Q_b + Q_f + \epsilon Q_i = 0. \qquad (28)$$

The flows here are the annual mean values. In Fig. 12 Q_a is plotted (negative values). As can be seen in the figure, Q_a is less than 0.1 Sv for the larger part of the parameter regime.

Using the calculated mean salinity gradient below the mixed layer (see Fig. 8) and the computed salt flux due to Atlantic inflow, it is possible to obtain an estimate of a "numerical" diffusion coefficient κ_n. With $Q_a = 0.1$ Sv, $\Delta S = 1.5‰$, $\Delta z = 100$ m and using $\kappa_n = Q_a S_a/(A\Delta S/\Delta z)$, one obtains $\kappa_n \approx 2 \times 10^{-5}$ m^2 s^{-1}. Comparing this value with estimates of diffusion coefficients in real systems κ_r, one finds that it is lower than, for example, values in the ocean thermocline where $\kappa_r \approx 1 \times 10^{-4}$ m^2 s^{-1} (see Broecker 1981). However, assuming $\kappa_r \sim N^{-1}$ (N: the buoyancy frequency) data published by Broecker (1981) indicate that $\kappa_r \approx 1 \times 10^{-5}$ m^2 s^{-1} when $N^2 \approx 1.5 \times 10^{-4}$ s^{-2}. This is the N^2 value one obtains using the above value of $\Delta S/\Delta z$. The numerical diffusion may thus be of the same order of magnitude as the diffusion in the real system.

5. Comparison with measurements

In order to compare the model stratification with field data, the seven stations shown in Fig. 1 were used. Horizontal means were calculated where each station was weighted with a representative area. The values of the integral quantities for each station together with the weighted means are presented in Table 2. In further discussion, error ranges for the integral quantities are needed. These were obtained by varying the representative areas of stations 6 and 7 between likely limits. Stations 6 and 7 were chosen because the difference in

TABLE 2. Values of HM, HD, SM and TM at each of the seven stations in Fig. 1 and weighted horizontal means with error ranges.

Station	HF (m)	HD ($\times 10^9$ J m^{-2})	SM ($\times 10^2$ m^2)	TM ($\times 10^4$ m^2)
1	6.97	1.63	4.71	7.75
2	9.21	1.77	6.33	8.53
3	10.62	1.76	8.56	9.14
4	11.91	2.05	9.38	11.9
5	8.32	1.63	3.65	5.11
6	4.68	1.88	3.23	11.2
7	15.29	1.95	12.2	11.2
Mean	9.5 ± 0.5	1.8 ± 0.1	7.2 ± 0.4	10.0 ± 0.5

TABLE 3. Model results for different Q_s when the total ice export $Q_{it} = 0.15$ Sv, $Q_b = 1.0$ Sv and $\lambda = 0.9$. The Q_i and Q_{is} are presented as percentage of the total ice export.

Q_s (Sv)	Q_i (%)	Q_{is} (%)	Q_g (Sv)	Q_a (Sv)	HF (m)	HD (J m^{-2})	SM (m^2)	TM (m^2)
0.0	100	0	1.0	0.06	9.0	$1.4 \cdot 10^9$	$6.5 \cdot 10^2$	$4.7 \cdot 10^4$
0.5	81	19	1.0	0.05	9.1	$1.6 \cdot 10^9$	$6.6 \cdot 10^2$	$6.8 \cdot 10^4$
1.0	56	44	1.0	0.04	9.2	$1.8 \cdot 10^9$	$6.7 \cdot 10^2$	$8.6 \cdot 10^4$
1.5	21	79	1.0	0.04	9.1	$2.0 \cdot 10^9$	$6.8 \cdot 10^2$	$9.7 \cdot 10^4$

HF is largest between these two. The error range in HF was estimated to be ±0.5 m or about ±5%. The same percentage error was then used for the other integral quantities. These ranges can be thought of as estimates of how well the actual state in the Arctic Ocean is known.

The difference between model and "observed" values of the four integral quantities should be within the error ranges of the observed quantities if this type of model could be said to simulate successfully the conditions in the Arctic. The mixed layer salinity and depth are not straightforward compared with field data because of the annual cycle of these properties. Many more stations from all seasons would be needed to establish monthly horizontal mean properties of the Arctic mixed layer. The result for the mixed layer will therefore be discussed in a more qualitative way.

Using the error ranges it is possible to construct areas in the Q_i, Q_b parameter plane where the model results are in agreement with the data. Such areas are shown for HF in Fig. 13, for $\lambda = 1$ and $\lambda = 2$. As can be seen in the figure the result is largely dependent on the outflow parameter λ. A λ value appropriate for the Arctic Ocean must therefore be chosen.

Here λ is assumed to depend on the number of "geostrophical outlets" γ and a slope parameter θ (defined below) such that $\lambda = \gamma\theta$. Stigebrandt (1981) estimated γ to be 2.3 assuming one full "geostrophical outlet" in the Fram Strait and one in Lanchaster Sound. The other channels in the Archipelago were estimated to represent 0.3 outlet together. A value of $\gamma = 2.3$ was found to fit in a two layer model but it is not sure that the value is the same in this continuous model. Calculating the total outflow using a mean profile of the seven profiles in Fig. 2 and using $\gamma = 2.3$ gives $Q_g = 2.4$ Sv.

Rudels (1987) calculated the transports of different water masses in Fram Strait and the Archipelago using measurements in Fram Strait together with continuity constraints for volume and salt, solving the inverse problem. These calculations gave 0.9 Sv through Fram Strait and 0.7 Sv through the Archipelago. The total outflow is then 1.6 Sv. Comparing this value with the 2.4 Sv above indicates that $\gamma = 2.3$ may be too large. Using Rudels transports and assuming one full outlet in the Fram Strait one obtains $\gamma = 1.8$. This lower value of γ will be adopted here because some facts are known about the conditions in the Archipelago (mentioned below) that favors a smaller γ than was suggested by Stigebrandt.

The water flowing through the Archipelago enters the Baffin Bay where the salinity is about 1‰ lower than in the Norwegian/Greenland Seas (Rudels 1986). This makes the density difference between the outflowing water and the reference density lesser in the Archipelago than in Fram Strait. The transport in a "geostrophic outlet" must then be lower there than in Fram Strait. Other factors suggesting that γ should be rather low is that the sill depth in Lanchaster Sound is only 125 m and land-fast ice is present in all channels during the larger part of the year. Stationary ice induces friction at the upper water surface which must reduce the transport.

Another important fact is that, when applying this model to the real system, the properties in the Arctic Ocean varies horizontally (see Fig. 2). The outflow parameterization is sensitive to this because the outflow from the Arctic Ocean must be driven by the density stratification in the outflow area and not by the horizontal mean stratification. This is accounted for by a slope parameter θ. In section 2 it was shown that the outflow is nearly proportional to SM. If station 5 is chosen to represent the properties in the outflow area it is the SM value at station 5, SM_5, that forces the outflow. Then θ can be defined as

$$\theta = (\overline{SM} + SM_5)/\overline{SM} \approx 0.5 \qquad (29)$$

where $\overline{SM}$ is the weighted mean of the seven stations. Choosing γ between 1.7 and 1.9 and using $\theta = 0.5$ one obtains $0.9 \leq \lambda \leq 1.1$. Thus, the area representing $\lambda = 1$ in Fig. 13 seems to be the one that is correct for the Arctic Ocean. Figure 13 can then be used to de-

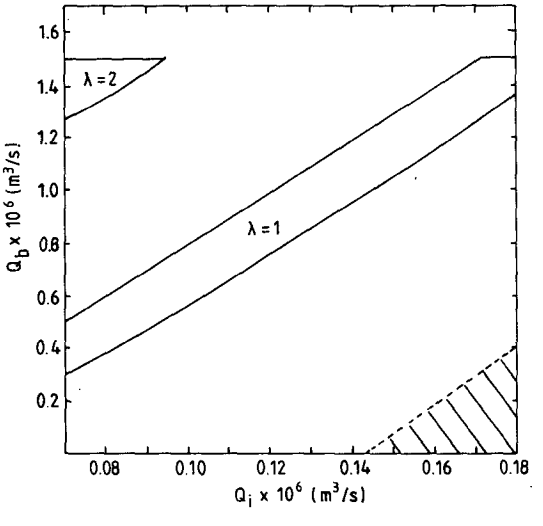

FIG. 13. The parameter areas for Q_i, Q_b that fulfill the condition HF = 9.5 ± 0.5 m, for $\lambda = 1$ and 2. Also shown is the area (shadowed) where the total outflow of freshwater from the system is greater than the supply.

termine if a certain Q_i, Q_b combination gives a "correct" HF. All combinations within the $\lambda = 1$ area give HF in the range of 9 ± 0.5 m obtained from field data. For example, Q_i, Q_b = (0.1, 1.5) Sv is not possible because this combination results in much too high freshwater content.

Looking at the other integral parameters (Fig. 10) for the case $\lambda = 1$, having in mind that Q_i, Q_b should be in the $\lambda = 1$ area, it is evident that SM will also fit the data if Q_i, Q_b is about (0.16, 1.3) Sv. However the situation does not look so good regarding the temperature parameters HD and TM. The HD will be too low unless Q_b is greater than 1.5 Sv, which seems unrealistic considering that the largest estimate found in the literature is 1.5 Sv and the latest investigations point towards Q_b less than 1 Sv. The situation is even worse looking at TM, which is totally impossible to get to agree with the measurements. The largest TM values generated by the model are only half of the values obtained from the measurements.

In order to test if the incorrectly low values of HD, SM and TM are caused by the relatively low diffusion below the mixed layer, a case with greater diffusion was tested. The greater diffusion was obtained by using nonzero κ in Eqs. (19) and (20). The result is shown in Fig. 14 where a case with small diffusion is shown together with a "large" diffusion case. For the Q_i, Q_b, λ combination used here all of the Bering Strait summer water has been entrained into the mixed layer resulting in no temperature maximum at all. The estimated diffusion coefficients are about 2×10^{-5} m^2 s^{-1} (only numerical diffusion) and 2×10^{-4} m^2 s^{-1}, respectively. Also shown are weighted mean temperature and salinity profiles from the seven stations in Fig. 2. This test shows quite clearly that increasing the diffusion is not the way to solve the problem. The larger diffusion increases the upward transport of heat making the temperature unrealistically high between about 75 and 250 m.

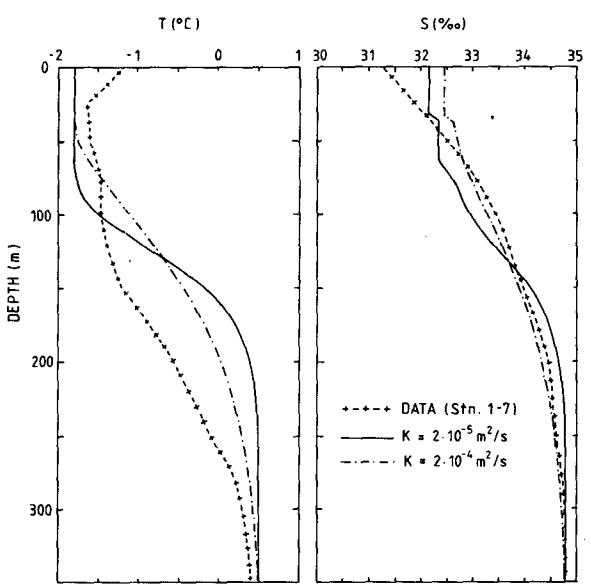

FIG. 14. Model generated (March) and observed (weighted horizontal mean of the seven stations in Fig. 2.) temperature and salinity profiles for a small diffusion (only numerical) and a larger diffusion. (Q_i, Q_b, λ) = (0.15 Sv, 1.0 Sv, 0.9).

This discrepancy between the model results and the data shows clearly that some important process or processes are missing in the model. The obvious candidate here is the hitherto omitted shelf circulation.

6. Model results when including shelf circulation

Both theoretical investigations and measurements have shown that the shallow Arctic shelves are able to produce water with high salinity and at freezing temperature (Aagaard et al. 1981; Melling and Lewis 1982). This water is then advected along the bottom into the central basin where it is interleaved at its appropriate density level.

This process will induce an internal circulation within the system, drawing surface water on to the shelf and returning more saline water at greater depths. In order to test how this type of circulation will influence the stratification in the basin, an experiment was run where a hypothetical shelf circulation was included in the model.

Practically, the inclusion of the shelf circulation was done by introducing a box (see Fig. 15) representing the shelf, which is allowed to exchange water with the original model. Mixed layer water enters the box and is transformed by ice production. The outflow from the box $q(S)$ is specified regarding temperature (at the freezing point) and the volume flux of water of different salinities. The outflowing water is interleaved in the main basin at its appropriate density level. The inflow to the box, Q_m, and the ice production in the box, Q_{is}, is calculated by continuity constraints for volume and salt to fit the prescribed outflow.

The outflow $q(S)$ is specified as a function of salinity according to Fig. 15. It seems realistic that most of the water produced on the shelf has a salinity that is slightly greater than S_m, and that just smaller amount of high salinity water is produced. The simplest $q(S)$ distribution that fulfills these specifications is linear, starting at S_m and decreasing towards higher salinities, becoming zero at some salinity S_s. The total volume flow from the shelf Q_s is then:

$$Q_s = \int_{S_m}^{S_s} q(S)dS \tag{30}$$

and the total outflow of salt ϕ is

$$\phi = \int_{S_m}^{S_s} q(S)SdS. \tag{31}$$

The continuity constraints for volume and salt then gives the inflow to the shelf Q_m and the amount of ice needed to be produced Q_{is}:

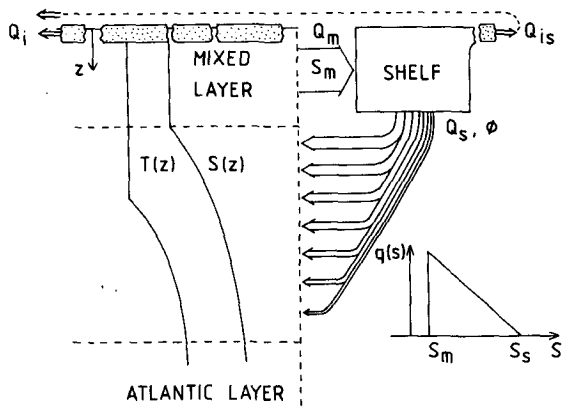

FIG. 15. Definition sketch of the hypothetical shelf. The outflow function $q(s)$ is also shown.

$$Q_m = (Q_s S_i - \phi)/(S_m - S_i) \tag{32}$$

$$Q_{is} = \frac{1}{\epsilon}(\phi - Q_s S_m)/(S_m - S_i). \tag{33}$$

This process is assumed to occur during the entire year with no seasonal variation. The ice produced on the shelf is added to the ice export from the interior basin such that the total ice export Q_{it} is

$$Q_{it} = Q_i + Q_{is}. \tag{34}$$

The experiment was run for $S_s = 34.55‰$ and several different values of Q_s. For each Q_s, different combinations of λ, Q_{it} and Q_b were tested. In order to obtain correct freshwater content the Q_{it}, Q_b combination was held approximately within the $\lambda = 1$ area in Fig. 13; λ was varied between 0.9 and 1.1. This result was then compared with the weighted mean temperature and salt profiles from the seven stations in Fig. 2 and the integral quantities. The best fit was obtained for $\lambda = 0.9$ and Q_{it}, $Q_b = (0.15, 1.0)$ Sv. The result in this case is shown in Fig. 16 for Q_s equal to 0, 0.5, 1.0 and 1.5 Sv. It should be noted that the total ice production is kept constant while the relative fraction of ice produced on and off the shelf will change according to Eq. (33).

The model results show that the shelf affects the system in several ways. Concerning the salt distribution, Fig. 16 shows that increasing Q_s makes the mixed layer fresher, the salinity just below the mixed layer increases and the salinity below about 150 m decreases. The behavior above 150 m is caused by the decrease in net ice production off the shelf and the increase in ice production on the shelf when Q_s increases. The salt supply to and the salinity of the mixed layer decreases when increasing Q_s. The salt that comes from the shelf ice production is injected below the mixed layer making this water more saline. Thus, the shelf causes a wider vertical distribution of the salt that comes from the total ice production. The percentages of the ice export that comes from the interior basin and the shelf respectively for different Q_s are presented in Table 3.

Most of the salt in the shelf outflow is injected close to the mixed layer due to the choice of the outflow function $q(s)$. About 75% of the salt flux in the shelf outflow occurs in the lower half ($S_m - S_s/2$) of the salinity range. An increase in Q_s will then tend to sharpen the halocline just below the mixed layer.

The decrease in salinity below about 150 m with increasing Q_s is caused by the temperature difference between the incoming cold shelf water and the surrounding water at that level. Due to its lower temperature the shelf water is injected at a level where the surrounding salinity is greater than in the shelf water.

The temperature is not affected by the shelf circulation above about 100 m because the temperature of this water is already at the freezing point. Below 100 m the temperature decreases with increasing Q_s and accompanying increasing injection of low temperature shelf water.

The case $Q_s = 0$ (no shelf circulation), is a case where the surface salinity is greater than the salinity of the Bering Strait inflow during part of the year. When Q_s is larger than about 1 Sv the water coming from the Bering Strait always enters below the mixed layer. It is injected in a narrow (about 30–45 m) depth interval. A consequence of this behavior is that the Bering Strait inflow contributes very little to the generation of the cold halocline when the shelf circulation is present.

Using Fig. 16 and the integral quantities (also in Table 3) it is now possible to estimate the magnitude of the shelf circulation in the Arctic Ocean. The best fit between the calculated curves and the profiles based on measurements seems to occur when Q_s is between 1.0 and 1.5 Sv. When Q_s is less than 1.0 Sv the tem-

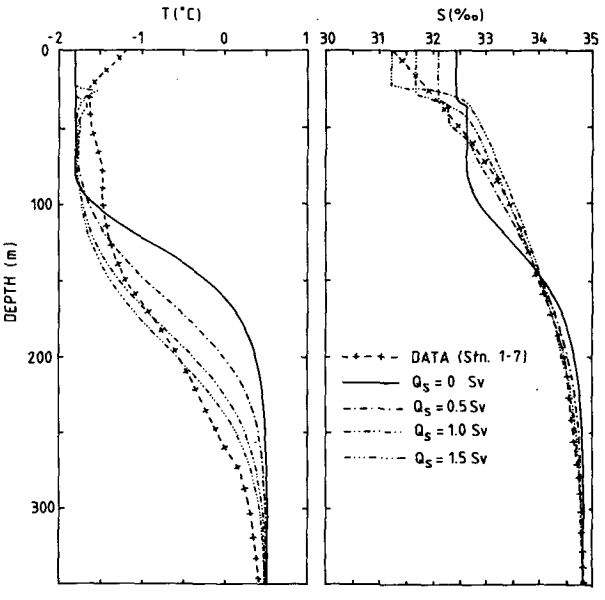

FIG. 16. Model generated and observed temperature and salinity profiles for (Q_{it}, Q_b) = (0.15, 1.0) Sv and different magnitude of the shelf outflow Q_s.

perature at low levels is too high and when Q_s is 1.5 Sv, or larger, the salinity just below the mixed layer is too high. The integral quantities (Table 3) shows a successively better agreement with increasing Q_s. The best fit here seems to be for Q_s = 1.5 Sv although HD in this case is slightly greater than the range obtained from the data. An estimate of the percentage of ice produced on the Arctic shelves can be obtained using a model result from Hibler (1979) showing the net ice production in the whole Arctic Basin. One finds that about 55% of the ice is produced on the shelf. In the present model calculation 44% of the ice is produced on the shelf when Q_s = 1 Sv and 79% when Q_s = 1.5 Sv. If Hibler is correct, the high percentage of ice produced on the shelf by the present model for the case Q_s = 1.5 Sv indicates that Q_s should be less than 1.5 Sv.

From this experiment one can draw the conclusion that an inflow of shelf water between 1 and 1.5 Sv, and with a linear salinity distribution as shown in Fig. 15 seems to give good agreement with the conditions in the real system. The calculated profiles and integral quantities are then close to field data. The percentage of ice produced on the shelf is in agreement with the result from Hibler's (1979) ice model. Furthermore the value of the ice export, 0.15 Sv, in this case is very near the most recent estimate by Vinje (1986), and the 1.0 Sv Bering Strait inflow also agrees with other estimates. Note also the quite realistic temperature maximum resulting from the Bering Strait summer water.

Also the mixed layer properties in this case seems to be in accordance with the data. The maximum mixed layer thickness is about 30 m and the minimum thickness is about 10 m. The mean salinity in the mixed layer is about 31‰ with a maximum of about 32‰ in winter and a minimum of about 30‰ in summer. These values seem to agree well with the data in Fig. 2.

The total outflow in this case is about 1.0 Sv (Table 3). It is hard to decide if this outflow is correct or not by comparing with figures obtained by other investigators because, for obvious reasons, these figures vary a lot. For example, Rudels (1987) obtained 1.6 Sv and Stigebrandt (1981) obtained 3.5 Sv.

It is certainly possible to refine this experiment further by, for example, varying the shape of the shelf outflow curve to obtain a nearly exact agreement with the measurements. However the actual state of the Arctic Ocean is not known well enough to justify a more sophisticated "curve fitting". It is also possible that part of the halocline structure is maintained by cooled and freshened inflowing Atlantic water from the Barents Sea instead of water participating in the shelf circulation. Rudels (1987) estimates that about 1.2 Sv of Atlantic water of salinity between 34.4 and 35‰ and temperature between +1° and −1.8°C enters via the Barents Sea.

7. Discussion and future outlook

The present model seems to explain several of the observed features of the Arctic Ocean. However, many problems still remain that deserve further investigation. For instance, the processes that generate the shelf circulation are not described at all in the present model. To do this, a separate shelf model is needed that generates the shelf outflow characteristics for a given forcing.

The chosen shelf outflow function, where the flow with the lowest salinity is interleaved just below the mixed layer, seems however to be quite realistic. Intrusions just below the mixed layer of shelf water at the freezing temperature have been observed in the Beaufort Sea (Melling and Lewis 1982). Concerning the shape of the outflow function it seems realistic that just small amounts of highly saline water can be produced on the shelves of the contemporary Arctic Ocean.

For creating a water mass of very high salinity, several conditions must be fulfilled: The initial salinity must not be too low. The water depth must not be too large. And last, the ice production over the water mass must be large during a sufficiently long time. It seems unlikely that all these conditions are fulfilled very often or in great areas on the shelf. The probability to create a water mass only slightly more saline than the mixed layer seems to be much larger.

By including a separate shelf model it would also be possible to describe the modification of the underlying Atlantic water by deep-reaching dense plumes from the shelves. This would make the Atlantic water active in the model. Thus, the model would in effect comprise the whole water column down to greatest depths. The present model only handles that part of the Atlantic water circulation that goes into the halocline by upward mixing (~0.04 Sv from the model). It is known that the total circulation of Atlantic water is much larger. Rudels (1987) estimates the total inflow of Atlantic water to about 1.2 Sv from the Barents sea and 1.9 Sv in the west Spitsbergen current. By extending the present model to include the whole water column it would be possible to study the whole circulation of Atlantic water as well as the deep and bottom water formation by very dense water coming from the shelf. Aagaard et al. (1985) show that the deep water in the Arctic Ocean appears to be a mixture of dense shelf water mixed with intermediate waters.

As mentioned earlier, a part of the cold halocline may be sustained by cold Atlantic water flowing across the Barents Sea. This inflow could easily be included in the model in the same way as the Bering Strait inflow. This extra source of cold water may provide an opportunity to increase the diffusion (and the outflow) with the cold halocline preserved. In order to distinguish between different origins of the water in the halocline, tracer data (for example, the oxygen isotope ratio $^{18}O/^{16}O$) may be useful.

Another problem that needs further analyses is the influence of the internal circulation in the basin on the outflow parameterization. In the Beaufort Sea a large gyre exists. The freshwater content in this anticyclonic gyre is larger than in the rest of the system (see station 7 in Fig. 2). This low salinity gyre water contributes greatly to the relatively low θ-value. It is quite possible that the stratification to a large extent within this gyre is maintained by its own circulation and does not respond directly to the outflow from the system. A way of dealing with this is to exclude the Beaufort gyre area when calculating horizontal means and θ.

In the present model, only the mass and salt budgets are considered. A logical next step in the modeling is to include the heat budget. The model should then include some parameterization of the heat fluxes to the atmosphere, whereby the ice production can be calculated instead of just being prescribed. In connection with the heat budget, it will also be important to analyze the heat flux from the Bering Strait.

Finally, it would be interesting to study the mixing below the mixed layer more in detail trying to achieve a better understanding of the involved mixing processes and their influence upon the state of the whole system. One process of particular interest here seems to be the mixing caused by entraining dense gravity currents coming from the shelves.

Acknowledgments. The author is indebted to Prof. Anders Stigebrandt for discussions of the present topics as well as for the channeling of funds from the Swedish Natural Science Research Council (NFR).

REFERENCES

Aagaard, K., and P. Greisman, 1975: Towards new mass and heat budgets for the Arctic Ocean. *J. Geophys. Res.*, **80,** 3821–3827.

——, L. K. Coachman and E. C. Carmack, 1981: On the halocline of the Arctic Ocean. *Deep Sea Res.*, **28,** 529–545.

——, A. T. Roach and J. D. Schumacher, 1985a: On the wind-driven variability of the flow through Bering Strait. *J. Geophys. Res.*, **90,** 7213–7221.

——, J. H. Swift, and E. C. Carmack, 1985b: Thermohaline circulation in the Arctic Mediterranean Seas. *J. Geophys. Res.*, **90,** 4833–4846.

Anderson, L. G., D. W. Dyrssen, E. P. Jones and M. G. Lowings, 1983: Inputs and outputs of salt, freshwater, alkalinity, and silica in the Arctic Ocean. *Deep-Sea Res.*, **30,** 87–94.

Broecker, W. S., 1981: Geochemical tracers and ocean circulation. *Evolution of Physical Oceanography,* B. A. Warren and C. Wunsch, Eds., MIT Press, 434–460.

Gill, A. E., and J. S. Turner, 1976: A comparison of seasonal thermocline models with observation. *Deep-Sea Res.*, **23,** 391–401.

Hibler, W. D., 1979: A dynamic thermodynamic sea ice model. *J. Phys. Oceanogr.*, **9,** 815–845.

Killworth, P. D., and J. M. Smith, 1984: A one-and-a-half dimensional model for the Arctic halocline. *Deep-Sea Res.*, **31,** 271–293.

Lemke, P., and T. O. Manley, 1984: The seasonal variation of the mixed layer and the pycnocline under polar sea ice. *J. Geophys. Res.*, **89,** 6494–6504.

Melling, H., and E. L. Lewis, 1982: Shelf drainage flows in the Beaufort sea and their effect on the Arctic Ocean pycnocline. *Deep-Sea Res.*, **29,** 967–985.

National Climatic Data Center (NCDC) Pilot chart data (TD-9757) in Selective Guide to Climatic Data Sources, U.S. Department of Commerce.

National Oceanographic Data Center (NODC), Oceanographic station data in NODC Users Guide, U.S. Department of Commerce.

Rudels, B., 1986: The outflow of polar water through the Arctic Archipelago and the oceanographic conditions in Baffin Bay. *Polar Res.*, **4,** 161–180.

——, 1987: On the mass balance of the Polar Ocean, with special emphasis on the Fram Strait. *Norsk Polarinstitutt Skrifter,* **188,** 1–53.

SCOR Working Group 58, 1979: The Arctic Ocean heat budget. Rep. No. 52, Geophys. Inst. Div. A., University of Bergen, Norway.

Stigebrandt, A., 1981: A model for the thickness and salinity of the upper layer in the Arctic Ocean and the relationship between ice thickness and some external parameters. *J. Phys. Oceanogr.*, **11,** 1407–1422.

——, 1985: A model for the seasonal pycnocline in rotating systems with application to the Baltic proper. *J. Phys. Oceanogr.*, **15,** 1392–1404.

——, 1987: Computations of the flow of dense water into the Baltic Sea from hydrographical measurements in the Arkona Basin. *Tellus,* **39A,** 170–177.

Thorndike, A. S., and R. Colony, 1982: Sea ice motion in response to geostrophic winds. *J. Geophys. Res.*, **87,** 5845–5852.

Treshnikov, A. F., and G. I. Baranov, 1973: Water circulation in the Arctic basin. Israel Program for Scientific Translations Ltd.

Vinje, T., and Ö. Finnekåsa, 1986: The ice transport through the Fram Strait. *Norsk Polarinstitutt Skrifter,* 186.